Journal of Innovative Optical Health Sciences
Vol. 3, No. 2 (2010) 131–134

DOI: 10.1142/S1793545810000940

WAVELET-BASED PALM VEIN RECOGNITION SYSTEM

QIANG LI, YAN'AN ZENG* and KUNTAO YANG
College of Optoelectronic Science and Engineering
Huazhong University of Science and Technology
Wuhan, 430074, P. R. China
**zya401@126.com*

A new personal recognition system using the palm vein pattern is presented in this article. It is the first time that the palm vein pattern is used for personal recognition. The texture feature of palm vein is extracted by wavelet decomposition. With our palm vein image database, we employed the nearest neighbor (NN) classifier to test the performance of the system. Experimental results show that the algorithm based on wavelet transform can reach a correct recognition rate (CRR) of 98.8%.

Keywords: Biometrics; wavelet transform; vein pattern.

1. Introduction

Many biometrics, such as the face, fingerprint, and iris images, have been studied extensively. In the last decade, hand vein-pattern biometrics has attracted increasing interest from both research communities[1–3] and industries.[4] Vein pattern is the vast network of blood vessels underneath a person's skin. The shape of vascular pattern is believed to be unique to each other in the corresponding part of the body and is very stable over a long period. Furthermore, vein patterns are harder for intruders to copy compared to other biometric features.

Wang *et al.* utilized the minutia features extracted from the vein patterns for recognition.[5] Im *et al.* employed a charge-coupled device (CCD) camera to capture vein-pattern images.[6] Wang *et al.* employed the multi-resolution wavelet analysis to extract the features in the hand vein image.[7] Whilst Fujitsu Laboratory has investigated the vein patterns in the palm side of the hand.[4]

To our knowledge, there is no institute or company has carried out research on palm vein patterns biometric recognition technology except for Fujitsu, but the features they used are not published in literature. In this article, we report on a wavelet-based palm vein recognition system. With our palm vein image database, we employed the nearest neighbor (NN) classifier to test the performance of the system.

2. Preprocessing of Palm Vein Images

2.1. *Image acquisition*

Biologically, there is a medical spectral window, which extends approximately from 700 to 900 nm, where the light in this spectral window penetrates deeply into tissues, thus allowing for noninvasive investigation.[8] In addition, the hemoglobin in venous blood absorbs more of the infrared (IR) radiation than the surrounding tissue.[1] Therefore, by shooting an IR light beam at the desired body part, an image can be captured using a CCD camera with an attached IR filter. In the resulted image, the vein patterns appear darker than the surrounding parts and are easily identifiable.

Since there is no palm vein pattern database available in public for research community, we design our own near IR palm vein image-acquisition system to utilize palm vein pattern for recognition. In this system, we use an array of light-emitting diodes (LEDs) that emit the IR light at a wavelength of 850 nm to shine IR light onto the palm side of the hand. At the same side, an IR CCD camera, of which the spectral response also peaks at a wavelength of around 850 nm, is used to obtain the image of the palm vein. To get rid of the effect by visible light, an IR filter is mounted in front of the lens of the camera.

With this system, we construct our own palm vein image database, which is about 50 individuals and consists of 1000 palm vein images from 100 different hands. The ages of these participants range from 18 to 60 years. Figure 1 shows a sample image from our database.

2.2. *Region of interest (ROI) extraction*

To increase the recognition accuracy and reliability, it is important to extract the features of vein patterns from the same region within different palm vein images. We select the second and fourth finger webs to fix the region that is defined as ROI. The procedures are stated as follows.

Step 1: The contour of the hand is extracted by thresholding. The result is shown in Fig. 2(b).

Step 2: For each point on the hand contour, the distance to the mid-point of the wrist is calculated, and then the four valley points between the fingers can be located. We can find the valley point between the thumb and forefinger as the distance between these points and the mid-point of the wrist is calculated. Then, the points P_1 and P_2 showed in Fig. 2(c) can be located.

Fig. 1. A palm vein images of hand in our database.

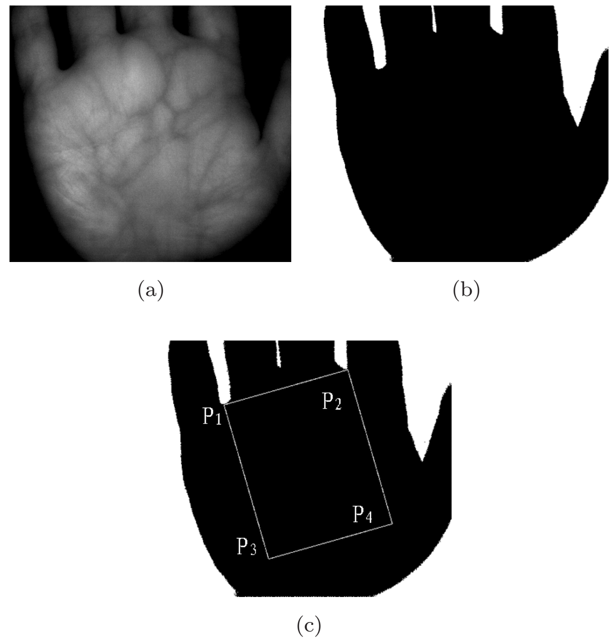

Fig. 2. Defining the ROI: (a) a palm vein image; (b) the palm region is made in binary format; and (c) locating the ROI.

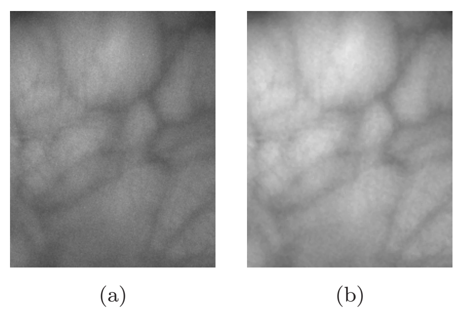

Fig. 3. ROI of the original image and the result of image enhancement: (a) ROI for the palm vein image; and (b) after noise reduction and normalization.

Step 3: With the points P_1 and P_2, the ROI is defined as a rectangular region P_1–P_2–P_3–P_4, where $l_{P_1P_3} = 1.25 \times l_{P_1P_2}$. Figure 3(a) shows the result of the extracted ROI for the palm vein image in Fig. 2(a).

2.3. *Image enhancement*

A 5×5 median filter is adopted to remove the speckling noise in the ROI image. Then normalization is performed to eliminate the disruption due to different illumination intensity and time. The normalization methods employed in this work are similar to those suggested by Hong *et al.*[9] Let $I(x, y)$ denote the intensity value at position (x, y)

in a vein-pattern image. The mean and variance of the image are denoted as μ and σ^2, respectively. Then, for an image with size $M \times N$, the normalized image $I'(x, y)$ is obtained using the pixel-wise operations in Eq. (1), where μ_d and σ_d^2 are the desired values for mean and variance, respectively; these two values are set empirically based on evaluation on numbers of sample images.

$$I'(x,y) = \begin{cases} \mu_d + \sqrt{\dfrac{\sigma_d^2 \cdot (\mathrm{I}(x,y) - \mu)^2}{\sigma^2}}, & \mathrm{I}(x,y) > \mu \\ \mu_d - \sqrt{\dfrac{\sigma_d^2 \cdot (\mathrm{I}(x,y) - \mu)^2}{\sigma^2}}, & \text{otherwise} \end{cases}. \tag{1}$$

Figure 3 shows the ROI of original image and the image after enhancement with noise reduction and normalization.

3. Wavelet Transform

Multi-resolution analysis enables the preservation of an image according to certain levels of resolution or blurring. Broadly speaking, multi-resolution analysis allows for the zooming in and out on the image. During the last two decades, wavelets theory has been widely used because wavelets provide a powerful tool for multi-resolution image analysis.

The discrete wavelet transform of $f(x)$ can be expressed as Eqs. (2) and (3).

$$W_\varphi(j_0, k) = \frac{1}{\sqrt{M}} \sum_x f(x) \varphi_{j_0,k}(x) \tag{2}$$

$$W_\psi(j, k) = \frac{1}{\sqrt{M}} \sum_x f(x) \psi_{j,k}(x), \tag{3}$$

where j is a scale parameter, k is a position parameter, $\varphi_{j,k}(x)$ is a scaling function, and $\psi_{j,k}(x)$ is the wavelet function.

The discrete wavelet transform of two-dimensional (2D) function $f(x, y)$ of size $M \times N$ is:

$$W_\varphi(j_0, m, n) = \frac{1}{\sqrt{MN}} \sum_{x=0}^{M-1} \sum_{y=0}^{N-1} f(x, y) \varphi_{j_0,m,n}(x, y) \tag{4}$$

$$W_\psi^i(j, m, n) = \frac{1}{\sqrt{MN}} \sum_{x=0}^{M-1} \sum_{y=0}^{N-1} f(x, y) \psi_{j_0,m,n}^i(x, y) \quad i = \{H, V, D\}, \tag{5}$$

where i represents the horizontal (H), vertical (V), or diagonal (D) direction. $W_\varphi(j_0, m, n)$ coefficients define an approximation of $f(x, y)$ at scale j_0. The $W_\psi^i(j, m, n)$ coefficients add horizontal, vertical, and diagonal details for scales $j \geq j_0$.

4. Wavelet-Based Palm Vein Recognition

Compared to other wavelets, Haar wavelet has the shortest supporting, which makes it better suitable for capturing the detail features of palm vein.[7] Therefore, in this work, the palm vein image was decomposed using three-level Haar wavelet. Figure 4 shows the Haar wavelet coefficients for the palm vein image in three levels of decomposition. In each level, we obtained an approximate image with low-frequency components and three detail images with high-frequency components in horizontal, vertical, and diagonal directions. These detail images reflect the texture feature of palm vein. Then, the approximate image was used in continuous decomposition. In the sub-images with scale 3, each wavelet sub-image was segmented into $n \times n$ blocks. The feature vector can be calculated by:

$$V_m = \frac{1}{N} \left(\sum_N |f_m(x, y) - M| \right) \quad m = 1, 2, \ldots, n^2, \tag{6}$$

where $f(x, y)$ is the gray value at position (x, y), m is the number of the blocks, N is the pixel number of each block, and M is the mean value of each block. Thereafter, the vector V can represent the

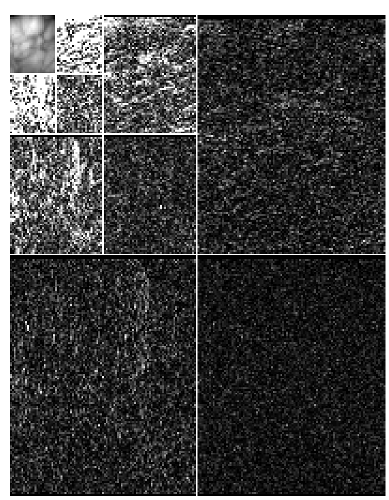

Fig. 4. Three-scale wavelet transform of the palm vein image.

palm vein feature.

$$V = [V_1, V_2, \ldots, V_{n^2}]. \tag{7}$$

In recognition stage, a simple NN classifier is employed. The correct recognition rate (CRR) is used to test the algorithm. Experimental results show the recognition rate can be as high as 98.8%.

5. Conclusion

In this article, we report on a wavelet-based palm vein recognition system. This system is more convenient to acquire vein images compared to those based on vein pattern of the back of the hand. A multi-resolution wavelet algorithm is employed to extract the features of palm vein patterns. Moreover, NN classifier is employed for the personal recognition. Experimental results show the algorithm reaches a recognition accuracy of 98.8%. It indicates that the wavelet decomposition is able to well represent the features of palm vein images.

References

1. J. M. Cross, C. L. Smith, "Thermo graphic imaging of subcutaneous vascular network of the back of the hand for biometric identification," in *Proceedings of IEEE 29th International Carnahan Conference on Security Technology*, Sanderstead, Surrey, England, p. 20 (1995).
2. S. K. Im, H. M. Park, S. W. Kim, C. K. Chung, H. S. Choi, "Improved vein pattern extracting algorithm and its implementation," in *IEEE International Conference on Consumer Electronics — Digest of Technical Papers*, Los Angeles, USA, p. 2 (2000).
3. C. L. Lin, K. C. Fan, "Biometric verification using thermal images of palm dorsa vein patterns," *IEEE Transactions on Circuits and Systems for Video Technology*, **14**, 199–213 (2004).
4. Fujitsu Laboratories Ltd., "Fujitsu Laboratories develops technology for world's first contactless palm vein pattern biometric authentication system," http://pr.fujitsu.com/en/news/2003/03/31.html, March 31 (2003).
5. L. Wang, G. Leedham, D. S.-Y. Cho, "Minutiae feature analysis for infrared hand vein pattern biometrics," *Pattern Recognit.* **41**, 920–929 (2008).
6. S. K. Im, H. M. Park, Y. W. Kim, S. C. Han, S. W. Kim, C. H. Hang, "An biometric identification system by extracting hand vein patterns," *J. Korean Phys. Soc.* **38**, 268–272 (2001).
7. Y. Wang, T. Liu, J. Jiang, "A multi-resolution wavelet algorithm for hand vein pattern recognition," *Chin. Opt. Lett.* **6**, 657–660 (2008).
8. S. Fantini, M. A. Franceschini, "Frequency-domain techniques for tissue spectroscopy and imaging," Chap. 7 in *Handbook of Optical Biomedical Diagnostics*, V. V. Tuchin, Ed., pp. 405–444, SPIE Press, Bellingham, WA (2002).
9. L. Hong, Y. Wan, A. Jain, "Fingerprint image enhancement: Algorithm and performance evaluation," *IEEE Transactions on Pattern Analysis and Machine Intelligence*, **20**, 777–789 (1998).